Fourier filtration of XANES as a source of quantitative information of interatomic distances and coordination numbers in crystalline minerals and amorphous compounds

L. A. Bugaev, A. P. Sokolenko, and H. V. Dmitrienko
Department of Physics, Rostov University, Zorge str., 5, Rostov-on-Don, 344090, Russia

A.-M. Flank
LURE, CNRS/CEA/MEN, Bat. 209D, B.P. 34, 91898 Orsay, France
(Received 20 April 2001; published 17 December 2001)

The method for quantitative determination of interatomic distances and coordination numbers (CN) in minerals and amorphous compounds by their x-ray absorption near edge structure (XANES) is proposed. The generation of the method and the proof of its main points are based on the revealed theoretical description of XANES for crystalline compounds and minerals as a sum of different photoelectron scattering processes on two- and approximately linear three-atoms chains, originated at the absorbing atom. The method consists of the Fourier filtration (FF) of the experimental XANES within the short range of photoelectron's wave numbers and the following fitting, with three varied parameters, of the first shell term extracted by the FF procedure. The accuracy of the obtained local structural parameters is illustrated for the reference crystalline minerals, which are used also to simulate the XANES formation in glasses. The application of the method to Mg XANES in diopside-glass and its crystalline equivalent, Diopside, permits one to determine the Mg-O distance and CN for the first oxygen shell around the Mg atom and to reveal the change of these parameters between the glass and the crystal with similar chemical composition.

DOI: 10.1103/PhysRevB.65.024105 PACS number(s): 61.10.Ht

I. INTRODUCTION

For a great number of poorly crystallized and amorphous compounds the x-ray absorption near edge structure (XANES) appears to be the most available source of information on their local atomic structure, when extended x-ray absorption fine structure (EXAFS) oscillations cannot be observed. However the analysis of the unknown structures by XANES provides now only indirect and qualitative information since it is usually performed comparing the XANES features of the compound studied with that of the reference ones.[1–5] One of the main problems here is to choose the appropriate references and to reveal for them the characteristic XANES features, which reflect the type of the atom's local environment. Thus, during last years the XANES of low-Z elements (Mg, Al, Si) in crystalline minerals, with known site symmetry and site occupancy, were studied extensively[6–9] and used as references for the XANES study of disordered compounds, such as glasses, clays, gels with similar chemical composition, where Mg, Al, and Si environments are unknown. The limitations of this approach are obvious and the origin of such a qualitative analysis arises from the traditional theoretical description of XANES in terms of the full multiple-scattering method.[10–13] This method permits one to reproduce the XANES features in agreement with the experiment for compounds with the known atomic structure, exactly determined by the diffraction methods, but appears to be of small use to solve the inverted problem—quantitative determination of local structural parameters, when the uncertainties in the diffraction data interpretation occur or these data are unavailable.

In this paper, to solve the inverted problem, the theoretical description of XANES is proposed, based on the treatment of the atom's absorption cross section in compound as a sum of different contributions from photoelectron scattering processes on the atoms of environment.[14] The validity of this description is proved via XANES calculations for a wide number of crystalline compounds and minerals, which consist of low-Z elements.[14,15] With its help the frequency separation of the first shell term from the others is revealed to be sufficient for applying the Fourier-filtration (FF) procedure to XANES and to extract the first shell term from the experimental spectrum. The fitting of the extracted term is performed within the short XANES range of photoelectron's wave numbers k to determine the structural parameters of polyhedron, which coordinates the absorbing atom (A) in the compound: R_1, the distance from A to the polyhedron's atoms and N_1, the coordination number (CN) of atom A. The proposed method for quantitative determination of local atomic structure by XANES, as well as the accuracy of the parameters R_1 and N_1 obtained by it, are illustrated for the reference crystalline minerals with different coordination of Al and Mg atoms using their Al and Mg XANES spectra. The application of this method to Mg XANES in diopside glass ($CaO\text{-}MgO\text{-}2SiO_2$) with unknown Mg local environment and in diopside crystal ($CaMgSi_2O_6$), permits one to obtain the R_1 and N_1 values and to reveal their changes between the glass and its crystalline equivalent.

II. THEORETICAL DESCRIPTION OF Al AND Mg XANES IN CRYSTALLINE COMPOUNDS AND MINERALS

The inverted problem—determination of structural parameters by XANES—can be solved within a method[14,15] which considers that the absorption cross section $\sigma(\varepsilon)$ of an

atom in compound is constituted of a sum of different photoelectron scattering contributions

$$\sigma(\varepsilon)=\sigma_{at}(\varepsilon)[1+\chi_{SS}^{(1)}(\varepsilon)+\chi_{SS}^{(MRO)}(\varepsilon)+\chi_{MS}(\varepsilon)], \quad (1)$$

where ε is the photoelectron energy started from the interstitial potential (EMT) called muffin-tin (MT) zero in the photon energy E scale, i.e., $\varepsilon=E-E_{MT}$; $\sigma_{at}(\varepsilon)$ is the factorized part of the absorption cross section, which contains the matrix element for $1s$ photoionization $|\langle 1s|\nabla|\varepsilon,p\rangle|^2$ and the contribution of the accompanied intrinsic processes within the absorbing atom. The $\chi_{SS}^{(1)}(\varepsilon)$ and $\chi_{SS}^{(MRO)}(\varepsilon)$ are the terms which correspond to the photoelectron single-scattering (SS) from the first shell and from the more distant shells [middle-range order (MRO) term], respectively.[14,15] The multiple scattering (MS) term $\chi_{MS}(\varepsilon)$ consists of the photoelectron double- and triple-scattering processes on atomic chains *A*-*F*-*S* originated at the absorbing atom *A* and chosen under the empirical ''selection rules,'' where *F* is the intermediate atom between *A* and *S*. The ''selection rules''[14] are obtained as a result of theoretical spectrum adjustment to the experimental one, performed by the SELCOMP code[14] which selects the scattering contributions from the two- and three-atoms chains, necessary to be considered for experimental spectrum description. These ''rules'' consist in the maximum value of scattering pathway length (R_{max}) on atomic chains and in the minimum value of angle parameter $C=|\cos(\overline{AF},\overline{AS})|$ for these chains. So the chains, considered for XANES calculations must have their C values within $C_{min}\leqslant C\leqslant 1.0$ and the scattering pathway length on them must be $\leqslant R_{max}$. The convergence of different MS terms, which results in the revealed ''selection rules,'' was discussed in Ref. 14.

The phase shifts for photoelectron scattering on atoms in the studied compounds were calculated using the method of Hartree-Fock (HF) MT-potential generation.[16] This method permits one to obtain theoretical XANES and EXAFS spectra systematically in agreement with the experimental ones[16–18] as well the high accuracy of structural parameters for the first shell, obtained from EXAFS data analysis, using the calculated phase shifts and scattering amplitudes.[19] Within this method the value of interstitial potential E_{MT} in the photon energy scale, used as the beginning for the photoelectron energy (ε) or wave number (k), was obtained, combining the vacuum level (VL) positions (E_{VL}) on the experimental spectrum and in the generated HF MT potential. As the result, the comparison of theoretical spectrum with the experimental one is performed under the coincident values of their VL. The E_{VL} on the experimental XANES was obtained according to the prescription of Ref. 16 and the E_{MT} position on the photon energy scale was determined then as $E_{MT}=E_{VL}-\varepsilon_{MT}$, where ε_{MT} is the VL position relatively to the MT zero. The value of the photon energy E which corresponds to the photoelectron energy ε was calculated by $E=E_{MT}+\varepsilon$. The accuracy of the obtained E_{MT} were tested everywhere comparing the theoretical and experimental XANES in the photon energy scale through the agreement of the main peaks energy positions as well as by the value of correlation coefficient, obtained within the comparison. In the following (Secs. III, IV) the obtained E_{MT} values are used also for the Fourier-filtration procedure.

Within the proposed method the accurate knowledge of the function $\sigma_{at}(\varepsilon)$ in the near edge region ($\varepsilon \leqslant 30$–50 eV) is important especially for the extraction of the first shell term $\chi_{SS}^{(1)}(\varepsilon)$ from the experimental XANES. However the MT approximation normally used, as well as the accounting for multielectron excitations—intrinsic losses only by the undetermined energy-dependent reduction factor $S_0^2(\varepsilon)$ (Ref. 20)—make unreliable the theoretical function $\sigma_{at}(\varepsilon)$, obtained through the direct *ab initio* calculations in the near edge energy region. Therefore the $\sigma_{at}(\varepsilon)$ was obtained from the experimental XANES spectrum of the compound studied by the generated procedure consists of the two steps. At first, the convolution of $\sigma^{exper}(\varepsilon)$ with the Lorentz function under the large, nonphysical value of its energy width Γ (the parameter used to account for the photoelectron inelastic losses and experimental resolution) is performed, which suppresses the oscillated χ terms in Eq. (1) and converts it into the parity $[\sigma^{exper}(\varepsilon)]_{convoluted}=[\sigma_{at}(\varepsilon)]_{convoluted}$, i.e., the $[\sigma_{at}(\varepsilon)]_{convoluted}$—the convoluted or ''smeared'' $\sigma_{at}(\varepsilon)$ is obtained from the experimental XANES spectrum by this step. The final step of the procedure is the solution of the inverted problem—the recovery of $\sigma_{at}(\varepsilon)$ from the $[\sigma_{at}(\varepsilon)]_{convoluted}$ under the used Γ value, performed by the generated recovery code.[21] The accuracy of the proposed procedure was tested for the studied reference minerals comparing their theoretical XANES with the experimental ones and comparing the values of local structural parameters, determined by $\sigma_{at}(\varepsilon)$, with the available diffraction data (Sec. III).

The photoelectron extrinsic losses were taken into account through the traditional exponential form $\exp[-R/\Lambda(\varepsilon)]$. The photoelectron mean free path length $\Lambda(\varepsilon)$ is usually not known exactly, especially for the near edge region of spectrum. However, the simulations of XANES, carried out with different $\Lambda(\varepsilon)$ dependencies, varied around the so-called universal curve for monatomic compounds[22] did not significantly change the obtained fine structure of spectrum. Therefore, smooth energy dependencies for $\Lambda(\varepsilon)$ were chosen for the direct XANES calculations so as to adjust the envelope of the experimental spectrum.

To account for the thermal atomic motion and the structure disorder in the studied compounds, every contribution into XANES from photoelectron scattering on atomic chains *A*-*S* or *A*-*F*-*S* was multiplied by the Debye-Waller (DW) factor $\exp(-2\sigma^2k^2)$. The XANES calculations were performed using the two different values of the DW parameter (σ^2): DW_1 for the first shell (oxygen polyhedron around the absorbing atom) and DW_2 for the more distant shells and MS terms. The validity of this approximation for crystalline minerals and glasses is justified via the direct calculations of their XANES spectra. These calculations show that under the ''reasonable'' values of the DW_1 parameter the obtained fine structures depend on the value of the ratio DW_2/DW_1. Therefore, considering for the arbitrary units of experimental intensities, this result permits to choose the value DW_1

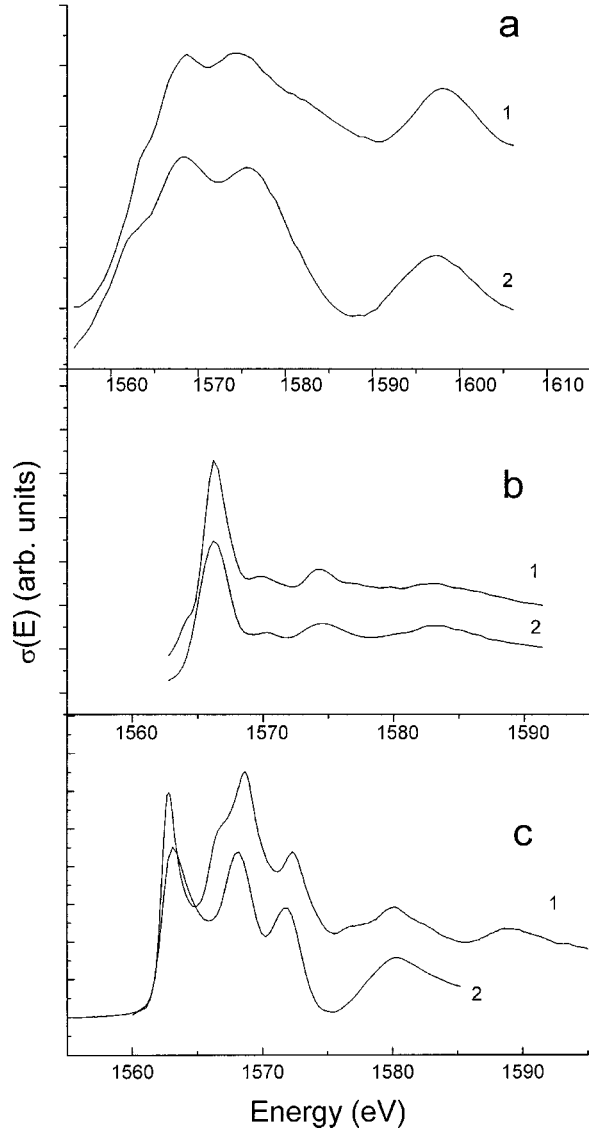

FIG. 1. Experimental (curves 1) and theoretical (curves 2) Al-XANES spectra of (a) Al-metal (CN=12); (b) berlinite (CN=4) and (c) AlN (CN=4).

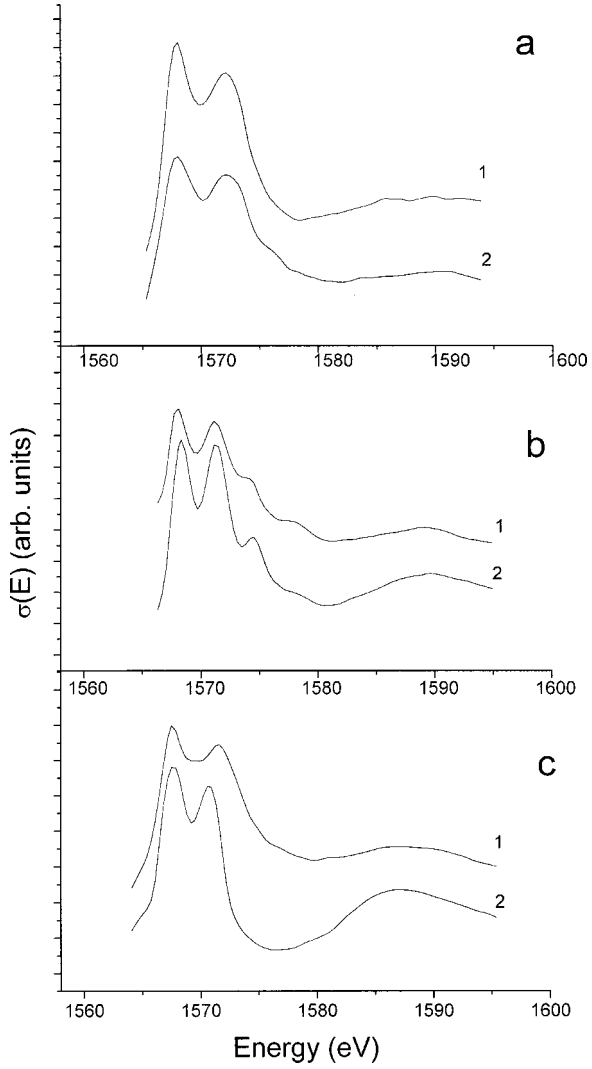

FIG. 2. Experimental (curves 1) and theoretical (curves 2) Al-XANES spectra of (a) *K*-alum (CN=6); (b) pyrophyllite (CN=6) and (c) diaspore (CN=6).

$=0.007$ Å^2 for the first shell in all crystalline minerals and diopside glass closely to the DW_1 values used for the complex oxides.[23] The choice of the DW_2 values for crystalline minerals will be discussed below in this section and for glasses in Sec. IV.

The experimental Al and Mg XANES for the reference crystalline compounds Al metal, AlN and crystalline minerals berlinite ($AlPO_4$), K alum [$KAl(SO_4)_2 12H_2O$], pyrophyllite [$Al_2Si_4O_{10}(OH)_2$], diaspore (α-AlOOH), spinel ($MgAl_2O_4$), pyrope ($Mg_3AlSi_3O_{12}$), and diopside ($CaMgSi_2O_6$) are presented in Figs. 1–3. The spectra of minerals exhibit the bright features at the energies $\varepsilon \leqslant 20$ eV above the absorption threshold and the following wide and broadened peaks, which rapidly decrease with the energy. The theoretical spectra, calculated through the proposed approach are compared with the experimental ones in the same Figs. 1–3. The comparison justifies the results of Refs. 14,15 and shows that the XANES of crystalline minerals composed of low-Z atoms are formed by the photoelectron SS processes and the double and triple scattering (MS) processes on the approximately linear three-atom chains originated at the absorbing atom, with the total pathway length R_{max} not exceeding ~ 18–20 Å. The calculations revealed the significant effect of the $\chi_{MS}(\varepsilon)$ term on the fine structure of spectrum within $\varepsilon \leqslant 15$–20 eV and show that the following features are formed mainly by $\chi_{SS}^{(1)}(\varepsilon)$ and less by $\chi_{SS}^{MRO}(\varepsilon)$ terms. The comparison of theoretical and experimental spectra within the energy region up to ~ 50 eV shows that their overall agreement is obtained when the DW_2 parameter for the second and more distant shells exceeds by ~ 7–8 times its value for the first shell (DW_1). Therefore the calculations were carried using the following DW parameters: $DW_1=0.007$ Å^2 and $DW_2=0.05$ Å^2. This ratio between the DW parameters for the first and more distant shells, obtained for the minerals, reflects the significant structure disorder in them and is expected to be stronger for amorphous compounds and glasses, where the second and

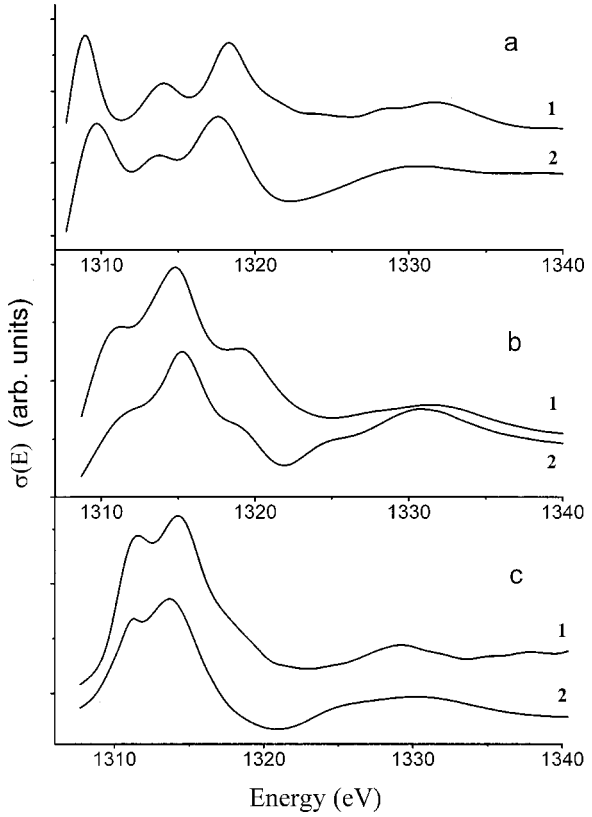

FIG. 3. Experimental (curves 1) and theoretical (curves 2) Mg-XANES spectra of (a) spinel (CN=4); (b) diopside (CN=6) and (c) pyrope (CN=8).

especially more distant shells are poorly formed and can be simulated under the large values of the DW parameters.[24]

III. THE FOURIER-FILTRATION OF XANES IN CRYSTALLINE MINERALS AND THE ACCURACY OF THE OBTAINED STRUCTURAL PARAMETERS

The revealed adequacy of the used XANES description permits one to consider the experimental absorption cross section of an atom in a compound as a sum of terms $\chi_{SS}^{(1)}(\varepsilon)$, $\chi_{SS}^{(MRO)}(\varepsilon)$, and $\chi_{MS}(\varepsilon)$, according to Eq. (1). The analysis of corresponding theoretical terms for the structures of reference minerals in Ref. 15 and in the present paper shows that the $\chi_{MS}(\varepsilon)$ is a high-frequency oscillated term (4–5 oscillations within the energy interval $\varepsilon \leqslant 30$ eV), while the term $\chi_{SS}^{(1)}(\varepsilon)$ is the low-oscillated one due to the small first shell radius $R_1 \sim 1.7$–2.2 Å. This frequency separation permits one to apply the Fourier transformation (FT) procedure to theoretical term $\chi_{SS}^{(1)}(\varepsilon)+\chi_{MS}(\varepsilon)$ within the short XANES k range: from $k_{min}=1.35$ to $k_{max}=2.8$ Å^{-1}. The FT result of the term $\chi_{SS}^{(1)}+\chi_{MS}$, calculated with the DW parameter $=0$ for berlinite and pyrophyllite structures, are presented in Fig. 4. The $|F(R)|$ for both structures are characterized by the presence of the broad first shell peak (up to ~ 4–5 Å) and the following structure, arises from the χ_{MS} term. The last conclusion is justified by the $|F(R)|$, obtained via FT of corresponding theoretical χ_{MS} terms only, also shown in Fig.

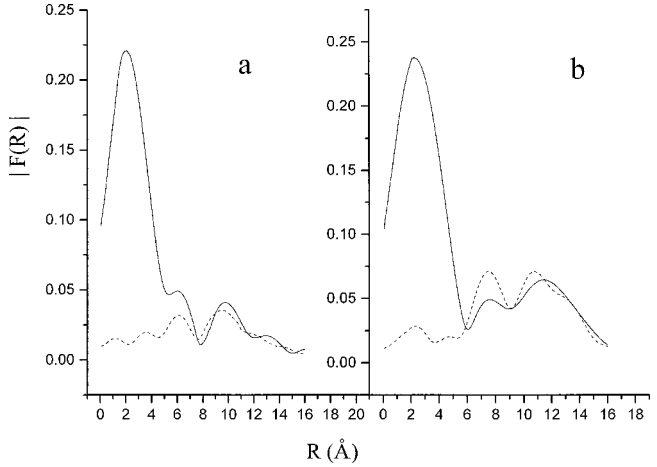

FIG. 4. $|F(R)|$ of theoretical functions $\chi_{SS}^{(1)}+\chi_{MS}$ (full curves) and χ_{MS} (dashed curves) for berlinite (a) and pyrophyllite (b).

4. As can be seen, the two main peaks in the $|F(R)|$ of χ_{MS}, except their small side lops at lower R values, are separated in R space from the first shell peak. Therefore, the back Fourier transformation (BFT) procedure, applied to the $|F(R)|$ of the sum $\chi_{SS}^{(1)}+\chi_{MS}$, with the window function at the first shell peak, permits one to extract the $\chi_{SS}^{(1)}$ term from this sum and to compare it with the initial theoretical one for the studied reference compounds. The comparison permits one to conclude that the small side lops of MS signal under the first shell peak in $|F(R)|$ does not affect significantly the accuracy of the Fourier filtration and hence can be ignored. The revealed separation in R space for the Fourier peaks which correspond to the terms $\chi_{SS}^{(1)}$ and χ_{MS} becomes more distinct when the DW factors are taken into account, especially under the obtained ratio between the DW parameters for the first and more distant shells in the studied minerals. In this case the affect of the χ_{MS} term on the determined R_1 and N_1, within the Fourier-filtration procedure, can be neglected.

At the same time the broad first shell peak in $|F(R)|$ overlaps the R region for the second and some more distant shells in spite of the strong enough separation between the radii of the first and the second shells (up to ~ 1 Å). Therefore, applying the BFT procedure to the $|F(R)|$ of the total function

$$\chi(\varepsilon)=\chi_{SS}^{(1)}(\varepsilon)+\chi_{SS}^{(MRO)}(\varepsilon)+\chi_{MS}(\varepsilon) \qquad (2)$$

with the window function up to ~ 4–5 Å, one must expect the extracted term $\chi_{SS}^{(1)}$, distorted by the presence of the $\chi_{SS}^{(MRO)}$-term contribution in this R region. In Ref. 15 the procedure for exclusion of the $\chi_{SS}^{(MRO)}$ affect on the extracted $\chi_{SS}^{(1)}$ term is proposed for crystalline minerals with uncertainties in the local atomic structure, arise from the ambiguity in the diffraction data interpretation. The proposed procedure is based on the approximately continuous distribution of the second and more distant shell's radii in these compounds, which permits to reproduce theoretically the $\chi_{SS}^{(MRO)}$ term for them. This reproduction can be performed under the uncertainties of ~ 0.3–0.4 Å in the values of the second and more distant shell's radii, using the unambiguous diffraction

data on the cell unit parameters and the type of symmetry. According to the prescription of Ref. 15 the subtraction of theoretically restored term $\chi_{SS}^{(MRO)}$ from the experimental absorption cross section $\sigma^{exper}(\varepsilon)$ by the rewritten Eq. (1):

$$\chi_{SS}^{(1)}+\chi_{MS}=\sigma^{exper}/\sigma_{at}-1-\chi_{SS}^{(MRO)} \quad (3)$$

permits one to extract the sum $\chi_{SS}^{(1)}+\chi_{MS}$ from the experimental XANES. The Fourier filtration of this function permits then to extract the first shell term $\chi_{SS}^{(1)}$ and to determine the corresponding structure parameters R_1 and N_1 applying the fitting procedure to the $\chi_{SS}^{(1)}$.

Simulations of the total theoretical function $\chi(\varepsilon)$ under the different values of the DW parameter for the second and more distant shells (DW_2) and the results of its Fourier filtration show that the affect of the $\chi_{SS}^{(MRO)}$ term on the extracted $\chi_{SS}^{(1)}$ rapidly decreases with the increasing of the DW_2 and becomes negligible when DW_2 exceeds by $\geqslant 10$ times DW_1—for the first shell. As will be shown in Sec. IV, such a ratio between the DW_2 and DW_1 must be used for glasses to simulate the poorly formed second and more distant shells in them. At the same time, for crystalline minerals which are characterized by the smaller difference between the DW_2 and DW_1 parameters (Sec. II) the term $\chi_{SS}^{(MRO)}$ can be the source of inaccuracies in the determined values of R_1 and N_1, i.e., applying the Fourier filtration to the total $\chi(k)$, the R_1 and N_1 are determined with the errors up to ~ 2 and $\sim 12\%$, respectively. Therefore for crystalline minerals the term $\chi_{SS}^{(MRO)}$ is theoretically recovered using the diffraction data on cell parameters and the type of symmetry and excluded from σ^{exper} according to Eq. (3). The results of Ref. 15 justified by the simulations of $\chi_{SS}^{(MRO)}$ term for the studied structures show that this recovery can be performed using the second and further shell's radii which can differ from their diffraction values by not more then ± 0.2 Å. In other words, the accuracy of R_1 and N_1 determined by the Fourier-filtration of the term $\chi^{theor}-\chi_{SS}^{(MRO)}$ remains the same as that obtained within the Fourier filtration of the term $\chi_{SS}^{(1)}+\chi_{MS}$, if the subtracted oscillation $\chi_{SS}^{(MRO)}$ is theoretically recovered using the approximate values for the second and further shells radii, known with the uncertainty of $\leqslant 0.3$–0.4 Å.[15]

The steps of the Fourier filtration applied to the experimental XANES of crystalline minerals berlinite and pyrophyllite with different coordination of the absorbing Al atom are illustrated in parts of Figs. 5(a)–(d) and 6(a)–(d). In (a) of each figure the experimental absorption cross section $\sigma^{exper}(\varepsilon)$ of the atom in the mineral is presented together with the obtained function $\sigma_{at}(\varepsilon)$. (b) shows the total function $\chi(\varepsilon)$ extracted from the $\sigma^{exper}(\varepsilon)$ by the rewritten Eq. (1): $\chi(\varepsilon)=\sigma^{exper}(\varepsilon)/\sigma_{at}(\varepsilon)-1$. (c) shows the result of the Fourier transformation $|F(R)|$ of the term $\chi-\chi_{SS}^{(MRO)}$. The final step of the Fourier filtration, the first shell term $\chi_{SS}^{(1)}$ obtained through the BFT of $|F(R)|$ with the window function at the first shell peak, is presented in (d) of the figures.

The structural parameters R_1 and N_1 of the oxygen polyhedron, which coordinates the absorbing Mg or Al atoms, are determined through the fitting of the extracted $\chi_{SS}^{(1)}$ term. The

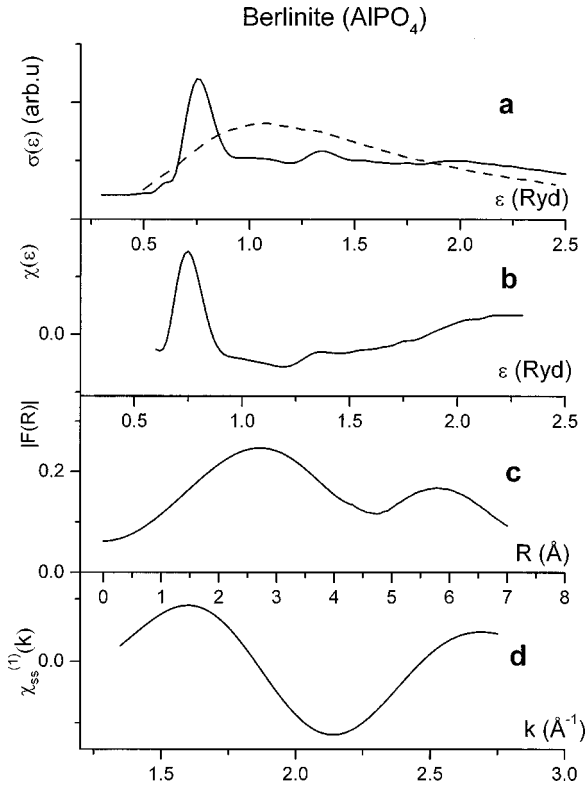

FIG. 5. The steps of the Fourier-filtration applied to the Al-XANES of berlinite: (a) $\sigma^{exper}(\varepsilon)$ and the obtained $\sigma_{at}(\varepsilon)$; (b) $\chi(\varepsilon)=\sigma^{exper}(\varepsilon)/\sigma_{at}(\varepsilon)-1$; (c) $|F(R)|$, the FT of $\chi-\chi_{SS}^{(MRO)}$; (d) the extracted first shell term $\chi_{SS}^{(1)}(k)$, the result of BFT applied to $|F(R)|$.

varied parameters for the fitting procedure are R_1, N_1, and Γ—the parameter for the core hole energy width and the experimental resolution account. The parameter Γ is varied within the exponential form $\exp(-0.2625\times 2R_1\Gamma/k)$ (Ref. 24) and the fitting is carried within the short range of the photoelectron wave numbers k from 1.35 to 2.8 Å^{-1}. Within this k interval the DW factor for the first shell $\exp(-2\times DW_1k^2)$ remains $\geqslant 0.9$ under the value $DW_1=0.007$ Å^2 used for the direct XANES calculations and therefore the same DW_1 value was taken and not varied. Within the fitting the reduction factor $S_0^2=1.0$ is used for the affect of intrinsic losses on the local density of electron's states on the absorbing atom.[25] At the same time, the affect of the intrinsic losses on the amplitude of the $|1s\rangle\rightarrow|\varepsilon p\rangle$ transition is automatically included in the atomic part of the absorption cross section $\sigma_{at}(\varepsilon)$ extracted from the experimental cross section $\sigma^{exper}(\varepsilon)$. The photoelectron scattering amplitudes and phase shifts for the fitting procedure were obtained within the same model of HF MT potential[16] used for the direct XANES calculations of Sec. II. As was mentioned there, the E_{MT} values used as the beginning for the wavenumber k, were determined for the studied compounds according to the HF MT potential generating procedure and therefore were not varied.

The results of the fitting (with three varied parameters R_1, N_1, and Γ) applied to the extracted term $\chi_{SS}^{(1)}$ are presented in Table I, where the R_1 and N_1 of the oxygen polyhedrons,

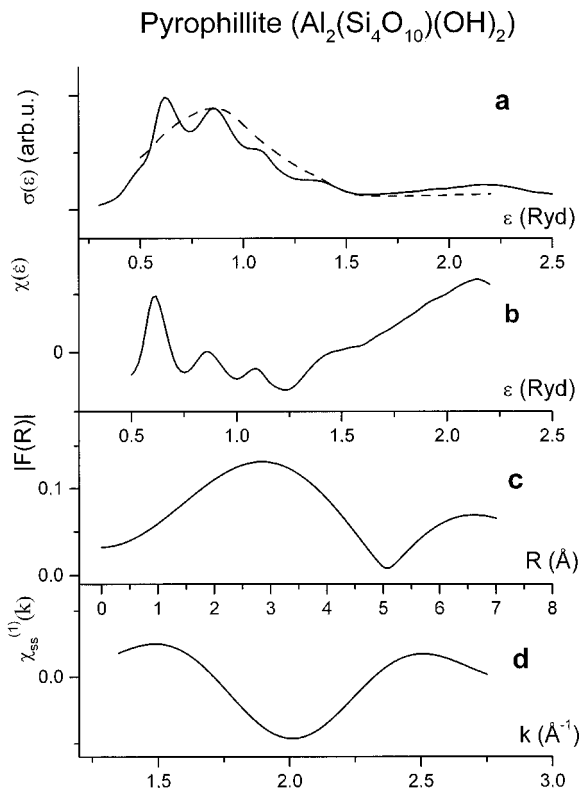

FIG. 6. The steps of the Fourier filtration applied to the Al-XANES of pyrophyllite: (a) $\sigma^{\text{exper}}(\varepsilon)$ and the obtained $\sigma_{at}(\varepsilon)$; (b) $\chi(\varepsilon)=\sigma^{\text{exper}}(\varepsilon)/\sigma_{at}(\varepsilon)-1$; (c) $|F(R)|$ the FT of $\chi-\chi_{\text{SS}}^{(\text{MRO})}$; (d) the extracted first shell term $\chi_{\text{SS}}^{(1)}(k)$, the result of BFT applied to $|F(R)|$.

which coordinates the Mg and Al atoms in the studied reference crystalline minerals, are compared with the available diffraction data. As can be seen the proposed Fourier filtration of experimental XANES and the following fitting procedure of the extracted first shell term permit to determine the R_1 and N_1 for metallic atoms environment in crystalline minerals with inaccuracy to $\leqslant 1\%$ and $\leqslant 3$–5%, respectively, under the values of parameter Γ within ~ 1–2.5 eV for all the reference compounds.

TABLE I. Structural parameters for the first oxygen shell in crystalline minerals, determined from the diffraction data and by the proposed method applied to their XANES.

Compound	Source	R_1 Å	N_1
Berlinite	diffraction (Ref. 26)	1.74	4
($AlPO_4$)	Al-XANES	1.74	3.9
Pyrophyllite	diffraction (Ref. 27)	1.91	6
[$Al_2Si_4O_{10}(OH)_2$]	Al-XANES	1.92	6.1
Diaspore	diffraction (Ref. 28)	1.91	6
($\alpha-AlOOH$)	Al-XANES	1.90	6.1
Spinel	diffraction (Ref. 29)	1.92	4
($MgAl_2O_4$)	Mg-XANES	1.93	3.9
Diopside	diffraction (Ref. 30)	2.07	6
($CaMgSi_2O_6$)	Mg-XANES	2.05	5.8
Pyrope	diffraction (Ref. 31)	2.19	8
($Mg_3AlSi_3O_{12}$)	Mg-XANES	2.17	7.9

The structure parameters R_1 and N_1 presented in Table I are obtained by the scattering amplitudes which need preliminary information of Al-O and Mg-O distances (R_1) used for their calculation. In the studied crystalline minerals the R_1 values for Al-O are changed by 0.18 from 1.74 Å in berlinite to 1.92 Å in pyrophyllite and for Mg-O by 0.27 from 1.92 Å in spinel to 2.19 Å in pyrope. Therefore the scattering amplitudes for the fit of $\chi_{\text{SS}}^{(1)}$ were calculated for the averaged R_1 values 1.83 Å for Al-O and 2.05 Å for Mg-O distances. At the same time, to reveal the effect of the inaccuracies in the input R_1 values on the obtained parameters R_1 and N_1, the following simulations were performed: (i) the $\chi_{\text{SS}}^{(1)}$ for berlinite was fitted by the scattering amplitudes, obtained at $R_1=1.92$ Å (as for pyrophylite) and (ii) the $\chi_{\text{SS}}^{(1)}$ for pyrophyllite was fitted by the scattering amplitudes obtained at $R_1=1.74$ Å (as for berlinite). The same procedure was performed for Mg-O distances between spinel and pyrope. The results of these simulations show that under the treated variations of the input R_1 values, typical for the wide row of the studied compounds, the errors in the determined R_1 and N_1 not exceed 1.5 and 5 %, respectively. However, when the R_1 values can differ strongly along the studied row of compounds, the effect of R_1 used for the scattering amplitudes calculation, on the obtained structure parameters must be studied additionally.

In general, the accuracy of the determined R_1 and N_1 depends also upon the choice of the beginning for the photoelectron wave numbers k—the argument of the scattering amplitudes and phase shifts used for the fit. Within the HF MT potential the values of E_{MT}—the beginning for k, were determined through the procedure[16] with the main points described in Sec. II. Nevertheless, to reveal the errors in R_1 and N_1 which can arise from the ambiguities in E_{MT} determination, the compulsory shifts of the obtained E_{MT} values by $\Delta E_{\text{MT}}=\pm 2.5$ eV (more than the typical shift of ~ 1 eV between the K-edge energy positions for the four- and six-coordinated Al or Mg atoms in the compounds) were made. The fit of the corresponding two functions $\chi_{\text{SS}}^{(1)}(k)$ obtained under two different values $E_{\text{MT}}\pm 2.5$ eV for the studied minerals shows the increase of errors in R_1 and N_1 determination—up to 3–4 and 10 %, respectively. This decrease of the accuracy justifies the importance of the efforts to propose the approaches which permit one to exclude the E_{MT} from the number of fitting parameters for compounds with arbitrary chemical composition.

IV. DETERMINATION OF LOCAL STRUCTURE PARAMETERS IN DIOPSIDE GLASS

In diopside glass (CaO-MgO-$2SiO_2$) the structure parameters R_1 and N_1 for the oxygen-polyhedron which coordinates the Mg atom are unknown. The comparison of Mg XANES in diopside glass with the Mg XANES in its crystalline equivalent diopside ($CaMgSi_2O_6$) presented in Ref. 9 shows that the glass spectrum retains all the main features of the crystal's spectrum, which are, however, strongly broad-

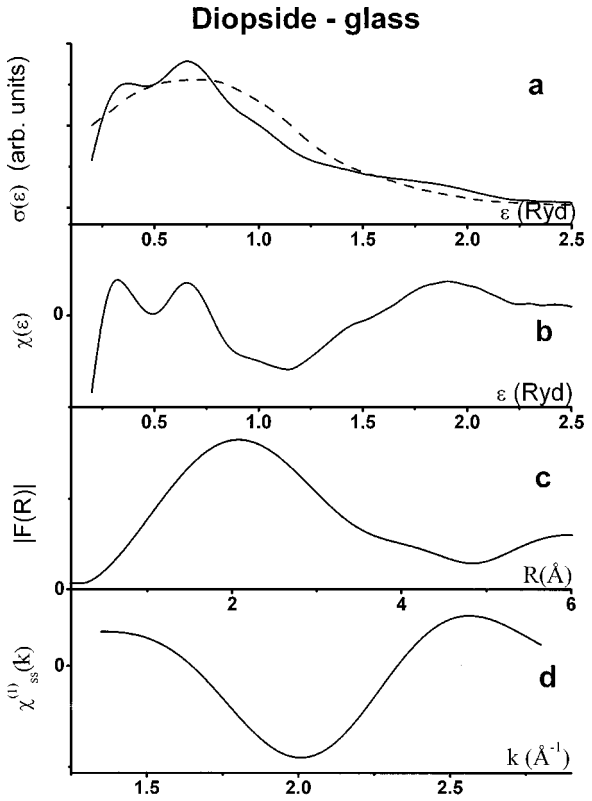

FIG. 7. The steps of the Fourier filtration applied to the Mg-XANES of diopside glass: (a) $\sigma^{\text{exper}}(\varepsilon)$ and the obtained $\sigma_{at}(\varepsilon)$; (b) $\chi(\varepsilon)=\sigma^{\text{exper}}(\varepsilon)/\sigma_{at}(\varepsilon)-1$; (c) $|F(R)|$, the FT of χ; (d) the extracted first shell term $\chi^{(1)}_{\text{SS}}(k)$, the result of BFT applied to $|F(R)|$.

ened. This broadening of XANES features between the glass and crystalline phases was also revealed in Ref. 32 for Ti-containing compounds and is induced by the structural disorder for the poorly formed second and especially more distant shells in glasses. As was mentioned in Sec. II, the effect of structural disorder on XANES can be accounted through the Debye-Waller-like damping, using the form $\exp(-2\times DWk^2)$ with the large values of the DW parameters for the second and more distant shells, DW_2. The simulations of XANES for the studied crystalline minerals with the varied DW_2 values for these shells and the fixed value of the DW_1 parameter for the first shell, reveal that the glasslike XANES structure is obtained under the ratio $\text{DW}_2/\text{DW}_1\geqslant 15$. At the same time the Fourier filtration of the theoretical XANES and the values of the parameters R_1 and N_1 determined by it, show that beginning from the ratio $\text{DW}_2/\text{DW}_1\geqslant 10$ (see Sec. III), the single scattering on the second and more distant shells—the term $\chi^{(\text{MRO})}_{\text{SS}}$ in $\chi(\varepsilon)$—weakly affect the obtained R_1 and N_1 values. Therefore one can conclude that the Fourier-filtration procedure can be applied directly to the XANES spectrum of amorphous compound providing the accurate R_1 and N_1 values, without the preliminary subtraction of the $\chi^{(\text{MRO})}_{\text{SS}}$ term from experimental $\chi(\varepsilon)$ as for crystalline ones.

The steps of the Fourier filtration of Mg XANES spectrum in diopside glass are presented in Figs. 7(a)–7(d). The fitting with the three varied parameters (R_1, N_1, and Γ) of the extracted first shell term $\chi^{(1)}_{\text{SS}}(k)$ permits one to obtain the Mg-O distance $R_1=2.12$ Å with $N_1=4.8$ oxygen neighbors around the absorbing Mg atom. This result is in agreement with molecular dynamics calculations[33] which predict mainly four- and five-coordinated Mg in a $MgSiO_3$ glass and with the estimations of Ref. 9 which indicate that Mg atoms in diopside glass are five-coordinated to oxygen atoms. At the same time, the obtained R_1 differ from the value $R_1=2.01$ Å derived from the poorly formed EXAFS of diopside glass.[9] The performed quantitative determination of local structural parameters using the Mg XANES spectra of diopside crystal and glass reveals hence the increase of the Mg-O distance from 2.07 Å in crystal to 2.12 Å in glass and finds the coordination number of Mg to be different in glass (CN=5) and in crystal (CN=6).

V. SUMMARY AND CONCLUSIONS

The proposed method for quantitative determination of structural parameters by XANES and the obtained results can be summarized as follows.

(i) The XANES of atom in crystalline minerals which consist of low-Z atoms ($Z\leqslant 20$) can be expanded in the sum of three terms: the photoelectron single scattering on the first shell ($\chi^{(1)}_{\text{SS}}$), the single scattering on the more distant shells ($\chi^{(\text{MRO})}_{\text{SS}}$), and the MS processes (χ_{MS}) on approximately linear three-atoms chains, originated at the absorbing atom.

(ii) The Fourier filtration of experimental XANES, performed for the short range of photoelectron's wave numbers k from 1.35 to 2.8 Å^{-1}, permits one to extract the first shell term $\chi^{(1)}_{\text{SS}}(k)$ distorted for crystalline minerals by the effect of the $\chi^{(\text{MRO})}_{\text{SS}}$ term within the first shell's Fourier peak. This distortion can appear to be the source of inaccuracies in the determined values of interatomic distances R_1 and coordination numbers N_1.

(iii) The preliminary subtraction of the term $\chi^{(\text{MRO})}_{\text{SS}}$, theoretically recovered according to the prescription of Ref. 15, from the experimental χ of crystalline minerals before its Fourier filtration, permits one to increase the accuracy of the obtained structural parameters R_1 and N_1.

(iv) For the studied reference minerals the interatomic distance R_1 and coordination number N_1 for the first shell, obtained through the fitting (with three varied parameters R_1, N_1, and Γ) of the term $\chi^{(1)}_{\text{SS}}(k)$ within the short XANES range of photoelectron wave numbers, are determined with inaccuracy to $\leqslant 1\%$ for R_1 and $\leqslant 3$–5% for N_1 under the values of Γ within ~ 1–2.5 eV.

(v) The experimentally observed broadening of the XANES features for glass compared to that for the related crystal can be described through the DW-like damping in the form $\exp(-2\times DWk^2)$ under the following ratio between the DW parameters for the first shell (DW_1) and for the poorly formed more distant shells and MS processes (DW_2): $\text{DW}_2/\text{DW}_1\geqslant 15$.

(vi) The simulations of XANES for the reference crystalline minerals revealed that under these values of the

DW_2/DW_1 ratio, the effect of $\chi_{SS}^{(MRO)}$ term on the determined R_1 and N_1 becomes negligible and hence the Fourier-filtration procedure can be applied directly to XANES of glass, providing the accurate values of its local structural parameters.

(vii) the application of the proposed method to Mg XANES spectra in diopside glass and its crystalline equivalent diopside revealed the increase of Mg-O distance from 2.07 Å in crystal to 2.12 Å in glass and found the coordination number of Mg to be different in glass (CN=5) and in crystal (CN=6).

This work was supported by Russian Foundation for Basic Research (RFBR) Grant No. 01-02-17013.

[1] G. S. Knapp, B. W. Veal, H. K. Pan, and T. Klippert, Solid State Commun. **44**, 1343 (1982).
[2] V. Maier and R. Frahm, Glastech. Ber. **62**, 20 (1989).
[3] C. S. Doyle, S. J. Traina, H. Ruppert, T. Kendelewicz, J. J. Rehr, and G. E. Brown, Jr., J. Synchrotron Radiat. **6**, 621 (1999).
[4] M. A. Castro, M. D. Alba, R. Alvero, A. I. Becerro, A. Munoz-Paez, and J. M. Trillo, J. Phys. (France) **7**, C2-827 (1997).
[5] Z. Zou, Y. F. Hu, T. K. Sham, H. H. Huang, G. Q. Xu, C. S. Seet, and L. Chan, J. Synchrotron Radiat. **6**, 524 (1999).
[6] Ph. Ildefonse, D. Cabaret, Ph. Sainctavit, G. Calas, A.-M. Flank, and P. Lagarde, Phys. Chem. Miner. **25**, 112 (1998).
[7] A. Marcelli, A. Mottana, G. Giuli, F. Scordari, and Z. Y. Wu, J. Phys. (France) **7**, C2-501 (1997).
[8] J. A. van Bokhoven, H. Sambe, D. C. Koningsberger, and D. E. Ramaker, J. Phys. (France) **7**, C2-835 (1997).
[9] Ph. Ildefonse, G. Calas, A.-M. Flank, and P. Lagarde, Nucl. Instrum. Methods **97**, 172 (1995).
[10] C. R. Natoli, D. K. Misemer, S. Doniach, and F. W. Kutzler, Phys. Rev. A **22**, 1104 (1980).
[11] R. V. Vedrinskii, L. A. Bugaev, I. I. Gegusin, V. L. Kraizman, A. A. Novakovich, S. A. Prosandeev, R. E. Ruus, A. A. Maiste, and M. A. Elango, Solid State Commun. **44**, 1401 (1982).
[12] F. J. Durham, J. B. Pendry, and C. H. Hodges, Comput. Phys. Commun. **25**, 193 (1982).
[13] S. J. Gurman, N. Binstead, and I. Ross, J. Phys.: Condens. Matter **17**, 143 (1984).
[14] L. A. Bugaev, Ph. Ildefonse, A.-M. Flank, A. P. Sokolenko, and H. V. Dmitrienko, J. Phys.: Condens. Matter **10**, 5463 (1998).
[15] L. A. Bugaev, Ph. Ildefonse, A.-M. Flank, A. P. Sokolenko, and H. V. Dmitrienko, J. Phys.: Condens. Matter **12**, 1119 (2000).
[16] L. A. Bugaev, R. V. Vedrinskii, I. G. Levin, and V. M. Airapetian, J. Phys.: Condens. Matter **3**, 8967 (1991).
[17] R. V. Vedrinskii, L. A. Bugaev, and V. M. Airapetian, J. Phys. B **24**, 1967 (1991).
[18] R. V. Vedrinskii, L. A. Bugaev, and I. G. Levin, Phys. Status Solidi B **150**, 307 (1988).
[19] R. V. Vedrinskii, L. A. Bugaev, and I. G. Levin, Physica B **158**, 421 (1989); L. A. Bugaev, V. A. Shuvaeva, K. N. Zhuchkov, E. B. Rusakova, and I. B. Alekseenko, J. Synchrotron Radiat. **6**, 29 (1999).
[20] J. J. Rehr, W. Bardyszewski, and L. Hedin, J. Phys. (France) **7**, C2-97 (1997).
[21] L. A. Bugaev, A.-M. Flank, A. P. Sokolenko and V. Yu. Grishkan (unpublished).
[22] L. C. Feldman and J. W. Mayer, *Fundamentals of Surface and Thin Films Analysis* (North-Holland, New York, 1986), p. 342.
[23] L. A. Bugaev, K. N. Zhuchkov, V. A. Shuvaeva, E. B. Rusakova, and R. V. Vedrinskii, J. Synchrotron Radiat. **8**, 308 (2001).
[24] I. B. Borovskii, R. V. Vedrinskii, V. L. Kraizman, and V. P. Sachenko, Usp. Fiz. Nauk **149**, 275 (1986).
[25] J. J. Rehr, J. Mustre de Leon, S. I. Zabinsky, and R. C. Albers, J. Am. Chem. Soc. **113**, 5135 (1991).
[26] D. Z. von Schwarzenbach, Kristallografiya **123**, 161 (1966).
[27] J. H. Lee and S. Guggenheim, Am. Mineral. **66**, 350 (1981).
[28] W. R. Busing and H. A. Levy, Acta Crystallogr. **11**, 798 (1958).
[29] P. Fisher, Z. Kristallogr. **124**, 275 (1967).
[30] P. Cameron, Am. Mineral. **58**, 594 (1973).
[31] N. Gibbs, Am. Mineral. **56**, 791 (1971).
[32] F. Fargees, G. E. Brown, and J. J. Rehr, Phys. Rev. B **56**, 1809 (1997).
[33] J. D. Kubicki, R. J. Hemley, and A. M. Hofmeister, Am. Mineral. **77**, 258 (1992).